Journal of Solid State Chemistry 184 (2011) 3110–3116

Contents lists available at SciVerse ScienceDirect

Journal of Solid State Chemistry

journal homepage: www.elsevier.com/locate/jssc

Evidence of a transition to reorientational disorder in the cubic alkali-metal dodecahydro-*closo*-dodecaborates

Nina Verdal [a,*], Hui Wu [a,b], Terrence J. Udovic [a], Vitalie Stavila [c], Wei Zhou [a,b], John J. Rush [a,b]

[a] NIST Center for Neutron Research, National Institute of Standards and Technology, Gaithersburg, MD 20899-6102, USA
[b] Department of Materials Science and Engineering, University of Maryland, College Park, MD 20742-2115, USA
[c] Sandia National Laboratories, Livermore, CA 94551-0969, USA

ARTICLE INFO

Article history:
Received 19 June 2011
Received in revised form
9 September 2011
Accepted 11 September 2011
Available online 22 September 2011

Keywords:
$B_{12}H_{12}^{2-}$
Dodecahydro-*closo*-dodecaborate
Neutron powder diffraction
Phase transition
Reorientational disorder

ABSTRACT

A neutron powder diffraction and differential scanning calorimetry (DSC) study indicates that $Cs_2B_{12}H_{12}$ undergoes a second-order phase transition near 529 K that can be described as a reorientational disordering of the $B_{12}H_{12}^{2-}$ icosahedral anions between two lowest-energy configurations within the cubic structure. Such a disordering requires the addition of another mirror plane to the low-temperature $Fm\bar{3}$ structural symmetry to become $Fm\bar{3}m$. Differential scanning calorimetry measurements suggest the possible persistence of some short-range anion order at and above the transition. Additional DSC measurements of the lighter alkali-metal cubic isomorphs, $Rb_2B_{12}H_{12}$ and $K_2B_{12}H_{12}$, also indicate second-order transitions for these compounds near 742 K and 811 K, respectively. These results are suggestive of similar order–disorder phase changes as for $Cs_2B_{12}H_{12}$, although confirmation of their existence requires analogous diffraction measurements.

Published by Elsevier Inc.

1. Introduction

The dodecahydro-*closo*-dodecaborate anion, $B_{12}H_{12}^{2-}$, is a physically and chemically intriguing molecular ion. In isolation, it is an undistorted, regular icosahedron, but it typically undergoes minor symmetry-breaking distortions when arranged among cations in an ionic lattice [1,2]. The inherently high kinetic stability of the icosahedral B_{12} cage makes it resistant to decomposition reactions at elevated temperatures, even in air [3]. In contrast, electrophilic B–H substitution reactions occur under relatively mild conditions justifying their description as three-dimensional aromatic species with highly delocalized bonding [4]. Current interest in this anion stems in part from its recognition as a by-product of the dehydrogenation of the light-metal tetrahydroborates [5] (e.g., $LiBH_4$), which are being investigated as potentially favorable hydrogen-storage materials. In this case, the high kinetic stability of the $B_{12}H_{12}^{2-}$ species is an unwanted attribute, since its formation and relative "inertness" hamper the ultimate hydrogen-storage capacity and reversibility of the parent tetrahydroborate materials [6]. Recently, the unknown room-temperature crystal structures of $Li_2B_{12}H_{12}$ (cubic, *Pa* symmetry) and $Na_2B_{12}H_{12}$ (monoclinic $P2_1/n$ symmetry) were determined [7,8] in an attempt to better understand the thermodynamic properties of these stable light-alkali-metal dodecahydro-*closo*-dodecaborate by-products. These somewhat unusual crystal structures, as compared to those previously established for the heavier alkali-metal analogs [3], are attributed to the much smaller cation radii of the two lightest alkali metals.

Indeed, all three heavier alkali-metal dodecahydro-*closo*-dodecaborate salts, $A_2B_{12}H_{12}$ (A=K, Rb, and Cs) with their relatively larger cations, were determined by single-crystal x-ray diffraction [3,9,10] to possess the same room-temperature cubic $Fm\bar{3}$ structure (see Fig. 1a). Such an ionic packing arrangement appears to be optimal for a cation radius above a threshold value between that of Na^+ and K^+. This sequence of heavier isomorphic dodecahydro-*closo*-dodecaborate salts was found to be fortuitous for investigating the effect of an increasing lattice size (without complicating structural changes) on $B_{12}H_{12}^{2-}$ rotational dynamics. Previous NMR and quasielastic neutron scattering (QENS) studies [11,12] have indicated that the $B_{12}H_{12}^{2-}$ anions in these heavier salts undergo measurable rapid rotational motions within the lattice with the motional frequency at a given temperature increasing with cation radius and unit-cell dimension. Such reorientational behavior is not uncommon for ionic solids that possess polynuclear cations or anions such as NH_4^+ or BH_4^-, and often leads to order–disorder-type structural phase transitions. For example, the propensity of the tetrahedral BH_4^- anions in the alkali-metal tetrahydroborates ABH_4 to undergo rotational reorientations [13–15] is typically accompanied by a second-order phase transformation [16,17] from a low-temperature ordered arrangement of BH_4^-

* Corresponding author. Fax: +301 921 9847.
E-mail address: nina.verdal@nist.gov (N. Verdal).

0022-4596/$ - see front matter Published by Elsevier Inc.
doi:10.1016/j.jssc.2011.09.010

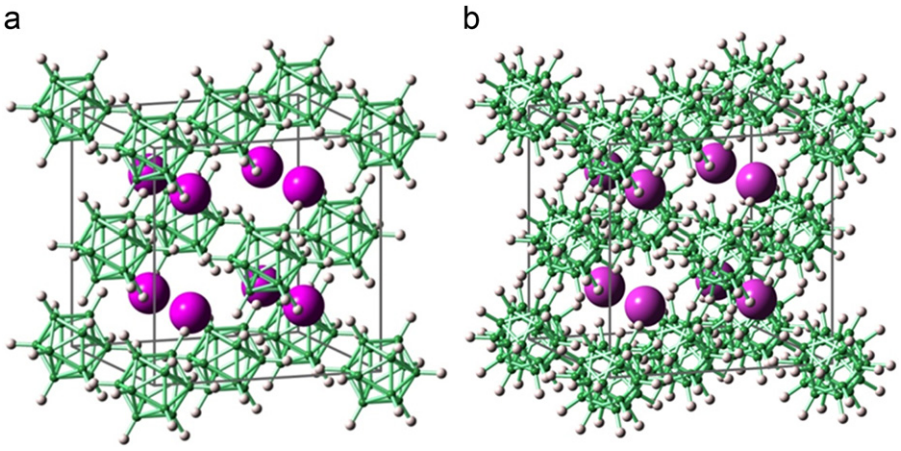

Fig. 1. (a) The low-temperature ordered $Cs_2B_{12}H_{12}$ cubic ($Fm\bar{3}$) structure. (b) The high-temperature disordered $Cs_2B_{12}H_{12}$ cubic ($Fm\bar{3}$m) structure. B, H (D), and Cs atoms are shown in green, white, and magenta, respectively. (For interpretation of the references to colour in this figure legend, the reader is referred to the web version of this article.)

anions (with 100% occupation of the four H crystallographic sites in a tetrahedral configuration around each B atom) to a high-temperature disordered arrangement (with a powder-diffraction average of 50% occupation of eight H crystallographic sites in a cubic configuration around each B atom). Although one might expect an analogous high-temperature transition to $B_{12}H_{12}^{2-}$ reorientational disorder for the cubic $A_2B_{12}H_{12}$ compounds, no phase change was recognized from prior DSC measurements [11] up to a temperature of 673 K. Nonetheless, in this paper, we show via a combination of neutron powder diffraction (NPD) and differential scanning calorimetry (DSC) that $Cs_2B_{12}H_{12}$ (and likely isostructural $Rb_2B_{12}H_{12}$ and $K_2B_{12}H_{12}$) indeed undergoes a phase transition involving a reorientational disordering of the $B_{12}H_{12}^{2-}$ anions (see Fig. 1b).

2. Experimental details

Isotopically enriched $Cs_2^{11}B_{12}H_{12}$ and $Cs_2^{11}B_{12}D_{12}$ (> 98% chemical purity, 99.5% ^{11}B isotopic purity) were purchased from Katchem [18]. Eliminating the highly neutron-absorbing ^{10}B isotope from the sample increases neutron transmission considerably. For NPD, D is preferable to H because the much larger H incoherent scattering cross section contributes substantially more to the non-Bragg background signal. In addition to the ^{11}B-enriched samples, $Cs_2B_{12}H_{12}$, $Rb_2B_{12}H_{12}$, and $K_2B_{12}H_{12}$ with natural-abundance B (80% ^{11}B, 20% ^{10}B) were prepared by previously published procedures [3,6,19]. Prior to experiments, any residual water was removed from all samples by evacuation at 573 K for 4 h. The resulting anhydrous materials were handled in a He-atmosphere glove box.

All measurements were performed at the NIST Center for Neutron Research. The NPD measurements were performed on the BT-1 High-Resolution Powder Diffractometer [20] at an incident neutron wavelength of 1.5401(2) Å with the Cu(3 1 1) monochromator and horizontal divergences of 60′, 20′, and 7′ of arc for the in-pile, monochromatic-beam, and diffracted-beam collimators, respectively. The wavelength was calibrated using a NIST Si standard reference material. The NPD patterns were collected from $Cs_2^{11}B_{12}D_{12}$ polycrystalline powder (3.6 g) contained in a Pb-gasket-sealed cylindrical V can (5 cm height × 1 cm diameter) over the 2θ range of 3–168° with a step size of 0.05°. The sample can was placed in a He closed-cycle refrigerator for both low-temperature and high-temperature measurements. Rietveld refinements [21] of the structure models were performed using the GSAS package [22]. Neutron scattering amplitudes used in the refinements were (5.42, 6.65, 6.67, and −3.74) fm for Cs, ^{11}B, D, and H, respectively [22]. Wavelength errors were not included in the standard deviations of the unit cells; i.e., the precisions reported in this paper for the structural parameters reflect the quality of the data and the corresponding refinement model, assuming a fixed neutron wavelength.

In addition to the structural measurements on the $Cs_2^{11}B_{12}D_{12}$ sample, neutron vibrational spectroscopy (NVS) and/or DSC with simultaneous thermogravimetric analysis (TGA) were performed on the various alkali-metal samples. The NV spectra were collected on the Filter-Analyzer Neutron Spectrometer [23] with the Cu(2 2 0) monochromator and horizontal divergences of 20′ of arc each for the in-pile and monochromatic-beam collimators. The simultaneous TGA and DSC were performed using a Netzsch (STA 449 *F1 Jupiter*) TGA-DSC under He flow with 3 mg to 11 mg samples, Al and/or Al_2O_3 sample pans, and temperature ramp rates upon heating ranging from 5 K/min to 10 K/min. The cooling rates were not controlled. Temperature readings were estimated to be accurate to within ±1 K.

3. Results and discussion

$Cs_2^{11}B_{12}D_{12}$ NPD patterns were collected at 24 K, 300 K, 470 K, 520 K, 550 K, and 580 K. Fig. 2 shows the $Cs_2^{11}B_{12}D_{12}$ patterns from 24 K to 520 K as well as the resulting model refinements. The fitted structural parameters for all temperatures are listed in Table 1. The patterns at 470 K and below agree well with the published $Fm\bar{3}$ structure [3]. In this arrangement (see Fig. 1a), the Cs^+ cations form a simple cubic sublattice. One $B_{12}D_{12}^{2-}$ anion resides at the center of every other cubic $(Cs^+)_8$ interstice, in an fcc sublattice arrangement of anions, and every anion possesses the same orientation. The anion orientation is such that each of the eight surrounding cations is able to interact equally with three of the twelve anionic D atoms in a tridentate fashion. Moreover, each D atom interacts equally with two of the cations. From the viewpoint of the cations, each is tetrahedrally surrounded by four anions, interacting with each anion in the same tridentate fashion. This suggests that the tridentate configurations maximize the favorable Coulombic interaction in this instance, as was shown to be the general case for the light-metal tetrahydroborates $M(BH_4)_n$ by *ab initio* calculations [24] of the isolated M^{n+} cations and BH_4^- anions.

Using the 24 K pattern and assuming that the D crystallographic sites were fully occupied with either D or H, we were able to determine an isotopic atom fraction D/(D+H) of 0.80,

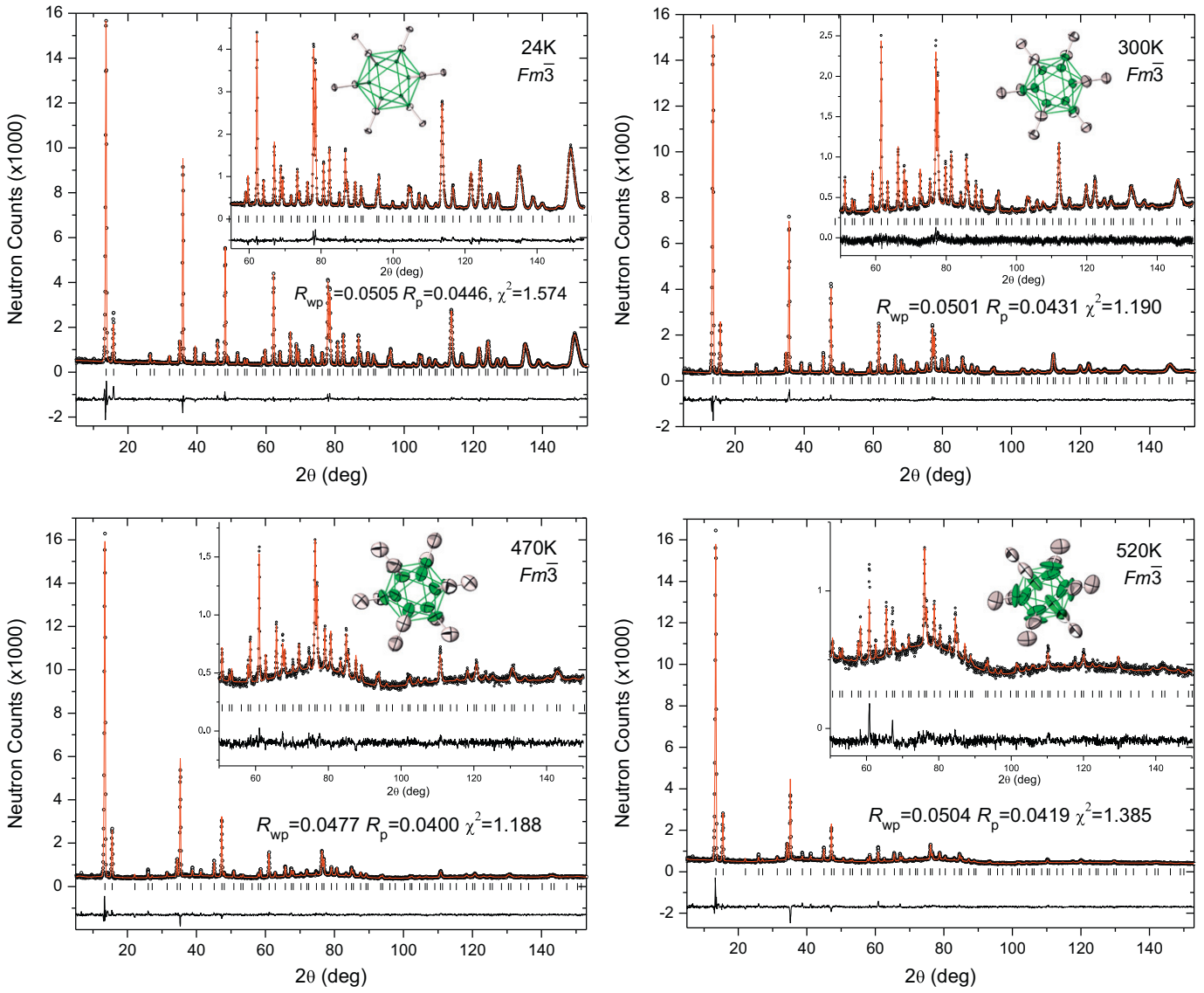

Fig. 2. Observed (circles), calculated (red lines), and difference profiles (beneath) of the Rietveld-refined NPD patterns for $Cs_2^{11}B_{12}D_{12}$ from 24 K to 520 K using the low-temperature $Fm\bar{3}$ structural model. Vertical bars denote the calculated Bragg peak positions. Uncertainties, not shown, are commensurate with the indicated scatter. In the insets, viewed down the [1 1 1] axis, are the corresponding anions defined by their thermal ellipsoids (green for B; white for D) resulting from the refinements. (For interpretation of the references to colour in this figure legend, the reader is referred to the web version of this article.)

implying that the stoichiometry of the sample as purchased was $Cs_2^{11}B_{12}(D_{0.8}H_{0.2})_{12}$. (The presence of H was corroborated by a comparison of the NV spectrum for this sample with that for $Cs_2^{11}B_{12}H_{12}$ [2]; see Fig. S1 in the Supplemental Information (SI)). Nonetheless, for the sake of simplicity, the sample will be referred to throughout as $Cs_2^{11}B_{12}D_{12}$.

Model refinements of the patterns at 24–520 K indicate increasingly elongated B and D thermal ellipsoids with increasing temperature (see Fig. 3), suggestive of a propensity for torsional displacements around the [1 0 0] axes as well as the [1 1 1] axes (see Fig. 4). By 520 K, the resulting ellipsoids are becoming more elongated, and the χ^2 value for the low-temperature structure model is just beginning to increase significantly. This suggests that the actual structure may be beginning to deviate from the model. By 550 K, the resulting ellipsoids from the low-temperature model are becoming overly elongated and aphysical, and the large χ^2 value indicates clearly that the model is no longer able to accurately fit the powder pattern (see Fig. 4). At this point, a good model fit to the data requires the addition of another mirror-plane symmetry element resulting in $Fm\bar{3}m$ symmetry. This has the effect of splitting the elongated B and D ellipsoids into two disordered positions with 50% occupancy (see Fig. 1b and Fig. 3). A comparison of the two different model fits to the 550 K data is shown in Fig. 4. Increasing to 580 K, the resulting pattern is still in good agreement with the $Fm\bar{3}m$ disordered model (see Fig. S2 in the SI).

The high-temperature structure can be described as a 90° reorientational disordering of the anions around the [1 0 0] axes of the cubic lattice. If one considers a single Cs_8-defined cube with an encaged $B_{12}D_{12}$ icosahedron, the additional mirror-plane symmetry element creates two different icosahedral orientations that would result in the same local low-energy configuration (with tridentate D_3–Cs interactions), except that one is the mirror image of the other. Whereas the low-temperature, ordered structure can be described as a coherent stacking of identically oriented (i.e., reorientationally aligned) interstitial icosahedra, the high-temperature, disordered structure can be described as an incoherent stacking (at random) of either of the two low-energy orientations described above. In other words, in the disordered structure, the choice between the two low-energy orientations for any particular anion no longer depends on the relative orientations of its neighboring anions.

Table 1
Refined structural parameters of $Cs_2^{11}B_{12}D_{12}$. The values in parentheses represent the standard deviation.

Atom	Site	Frac.	x	y	z	U_{11}	U_{22}	U_{33}	U_{12}	U_{13}	U_{23}
(a) 24 K: a=11.15730(9) Å (space group $Fm\bar{3}$, No. 202). R_{wp}=0.0505 R_p=0.0446 χ^2=1.574											
Cs	*8c*	1.0	0.25	0.25	0.25	0.69(5)	0.69(5)	0.69(5)	0	0	0
B	*48h*	1.0	0	0.1288(1)	0.0798(1)	0.83(4)	0.66(5)	1.07(5)	0	0	−0.14(3)
D	*48h*	1.0	0.1990(8)	0.2201(1)	0.1366(2)	1.07(8)	0.26(6)	0.78(7)	0	0	−0.25(6)
(b) 300 K: a=11.2589(1) Å (space group $Fm\bar{3}$, No. 202). R_{wp}=0.0501 R_p=0.0431 χ^2=1.190											
Cs	*8c*	1.0	0.25	0.25	0.25	2.98(9)	2.98(9)	2.98(9)	0	0	0
B	*48h*	1.0	0	0.1283(1)	0.0797(1)	3.50(8)	2.87(8)	3.20(8)	0	0	−0.23(6)
D	*48h*	1.0	0.2000(9)	0.2197(1)	0.1343(1)	3.7(1)	1.75(9)	3.0(1)	0	0	−1.14(9)
(c) 470 K: a=11.3482(2) Å (space group $Fm\bar{3}$, No. 202). R_{wp}=0.0477 R_p=0.0400 χ^2=1.188											
Cs	*8c*	1.0	0.25	0.25	0.25	5.4(2)	5.4(2)	5.4(2)	0	0	0
B	*48h*	1.0	0	0.1246(2)	0.0791(2)	4.7(1)	4.7(1)	5.9(1)	0	0	−2.1(1)
D	*48h*	1.0	0	0.2128(4)	0.1348(5)	4.7(2)	5.4(2)	5.5(2)	0	0	−1.6(1)
(d) 520 K: a=11.3852(3) Å (space group $Fm\bar{3}$, No. 202). R_{wp}=0.0504 R_p=0.0419 χ^2=1.385											
Cs	*8c*	1.0	0.25	0.25	0.25	8.4(3)	8.4(3)	8.4(3)	0	0	0
B	*48h*	1.0	0	0.1179(4)	0.0847(5)	4.6(2)	10.7(4)	11.9(3)	0	0	−8.2(2)
D	*48h*	1.0	0	0.2086(6)	0.1367(6)	3.4(3)	8.9(3)	8.5(4)	0	0	−3.6(3)
(e) 550 K: a=11.4125(3) Å (space group $Fm\bar{3}m$, No. 225). R_{wp}=0.0380 R_p=0.0315 χ^2=1.196											
Cs	*8c*	1.0	0.25	0.25	0.25	7.0(2)	7.0(2)	7.0(2)	0	0	0
B	*96j*	0.5	0	0.1272(2)	0.0784(2)	5.6(2)	5.7(2)	6.3(3)	0	0	−0.9(1)
D	*96j*	0.5	0	0.2154(4)	0.1331(3)	6.8(3)	3.8(2)	6.4(2)	0	0	−3.4(2)
(f) 580 K: a=11.4197(2) Å (space group $Fm\bar{3}m$, No. 225). R_{wp}=0.0294 R_p=0.0244 χ^2=1.214											
Cs	*8c*	1.0	0.25	0.25	0.25	6.7(1)	6.7(1)	6.7(1)	0	0	0
B	*96j*	0.5	0	0.1253(1)	0.0767(1)	5.4(1)	4.5(1)	5.2(2)	0	0	−1.2(1)
D	*96j*	0.5	0	0.2146(2)	0.1315(2)	9.7(2)	8.5(2)	10.6(2)	0	0	−2.3(2)

The resulting NPD pattern reflects the two superimposed anion configurations (see Fig. 5). This type of disorder is analogous to that mentioned earlier for the alkali-metal tetrahydroborates, where the second mirror plane of the $Fm\bar{3}m$ symmetry allows for the superposition of two BH_4^- tetrahedra (again differing by a 90° reorientation) to form an overall disordered cubic arrangement of H atoms. Yet, for this particular structural arrangement, a bidentate interaction between all BH_4^- anions and alkali-metal cations turns out to be the most favorable configuration, contrary to the tridentate interaction favored for the case of an isolated anion and cation (*vide supra*).

It should be noted from the NPD patterns in Figs. 2 and 4 that there is an increasing amount of diffuse scattering with increasing temperature (e.g., the broad background peak maximized near 76° 2θ, enhanced in the insets). This is attributed to the increasing dynamic disorder scattering of the librating $B_{12}D_{12}^{2-}$ icosahedra with increasing temperature (as evidenced by the elongating thermal ellipsoids), analogous to what is observed [25] in solid C_{60} below its rotational melting transition. No effort was made to predict the exact functional form of this scattering, since it is complicated by the supposedly random substitution of some of the D atoms in the $Cs_2^{11}B_{12}D_{12}$ sample with H atoms.

To further characterize the nature and location of the phase transition, NPD data were collected for an expanded series of temperatures over a more limited 2θ region (~75–79°; see Fig. 6b). One striking change in the diffraction pattern with temperature is in the ratio of the peak areas of a doublet found in this region. At 24 K, the areas of the peaks at 77.9° and 78.4° are nearly equal. Yet, as the temperature is increased, the peaks shift to lower angle and the ratio of higher-angle to lower-angle peak areas drops slowly at first up to 500 K, then more rapidly to zero between 500 K and 540 K, suggesting that a second-order structural phase transition occurs within this region and is complete by 540 K (Fig. 6). Based on the size and mass of the NPD sample, we cannot rule out the presence of a minor temperature gradient (of a few degrees K) across the sample causing some smearing out of the phase transition.

We used DSC measurements to provide further evidence and details of the phase transition. The DSC of fully protonated $Cs_2^{11}B_{12}H_{12}$ (see Fig. 7) shows a second-order phase transition (15–20 K in width) at 529 K (the onset of the transition peak upon heating at 10 K/min). The DSC of $Cs_2B_{12}H_{12}$ (with natural-abundance B, not shown) yielded a similar result, as expected. The DSC of the deuterated $Cs_2B_{12}D_{12}$ material used for NPD yields a slightly lower phase-transition temperature of 527 K, indicating a minor isotope effect. This transition temperature is marked by a vertical line in Fig. 6a. Again, the DSC data corroborate the NPD results, pointing to a phase transition that begins above ≈500 K and ends by ≈540 K. The observation of a DSC transition contradicts a previous study [11] that reported no phase transition in this temperature regime, although a close inspection of a prior DSC measurement [3] of $Cs_2B_{12}H_{12}$ by the same authors indeed shows an (unmentioned) extremely weak feature near the transition temperature found in the present study. Analogous, somewhat stronger DSC features were also evident [3,26] at 557 K, 639 K, 739 K, and 729 K for the mixed-anion compounds $Cs_3IB_{12}H_{12}$, $Cs_3BrB_{12}H_{12}$, $Cs_3ClB_{12}H_{12}$, and $Rb_3BrB_{12}H_{12}$, respectively, which may very well reflect similar order–disorder transitions involving the $B_{12}H_{12}^{2-}$ anions. Although no NPD measurements were performed on the isomorphic $Rb_2B_{12}H_{12}$ and $K_2B_{12}H_{12}$ compounds, DSC measurements (see Fig. 8) indeed show that transitions were also observed for $Rb_2B_{12}H_{12}$ at 742 K (the onset of the peak upon heating 10 K/min), and for $K_2B_{12}H_{12}$ at 811 K. (N.B., $K_2B_{12}H_{12}$ was heated momentarily up to 846 K without extensive decomposition before the cooling measurement, although this is probably above the practical thermal limit of the compound.) It should be noted that an increase in the observed transition temperature going from $Cs_2B_{12}H_{12}$ to $Rb_2B_{12}H_{12}$ to $K_2B_{12}H_{12}$ correlates with their decreasing room-temperature cubic lattice constants of 11.2812(7) Å, 10.8674(8) Å, and 10.6290(8) Å, respectively [3]. Thus, the relative behavior of these DSC measurements suggests that both $Rb_2B_{12}H_{12}$ and $K_2B_{12}H_{12}$ undergo a similar order–disorder phase transition as $Cs_2B_{12}H_{12}$.

During the DSC measurements, the accompanying TGA indicated no significant mass losses, consistent with the observed reversibility of all the transitions during thermal cycling. From a comparison of the areas of the integrated DSC transition peaks

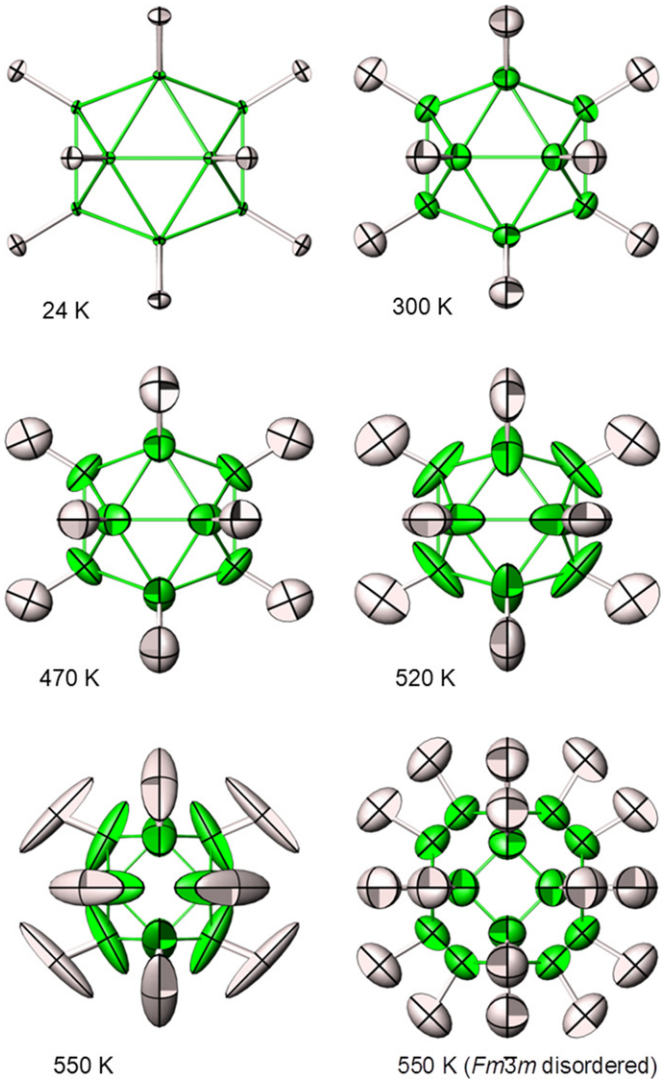

Fig. 3. Viewed down the [1 0 0] axis, the $B_{12}D_{12}$ icosahedra from $Cs_2^{11}B_{12}D_{12}$ defined by their thermal ellipsoids (green for B; white for D) resulting from the low-temperature, ordered $Fm\bar{3}$ structural model (24 K to 550 K) and high-temperature, disordered $Fm\bar{3}m$ structural model (550 K). (For interpretation of the references to colour in this figure legend, the reader is referred to the web version of this article.)

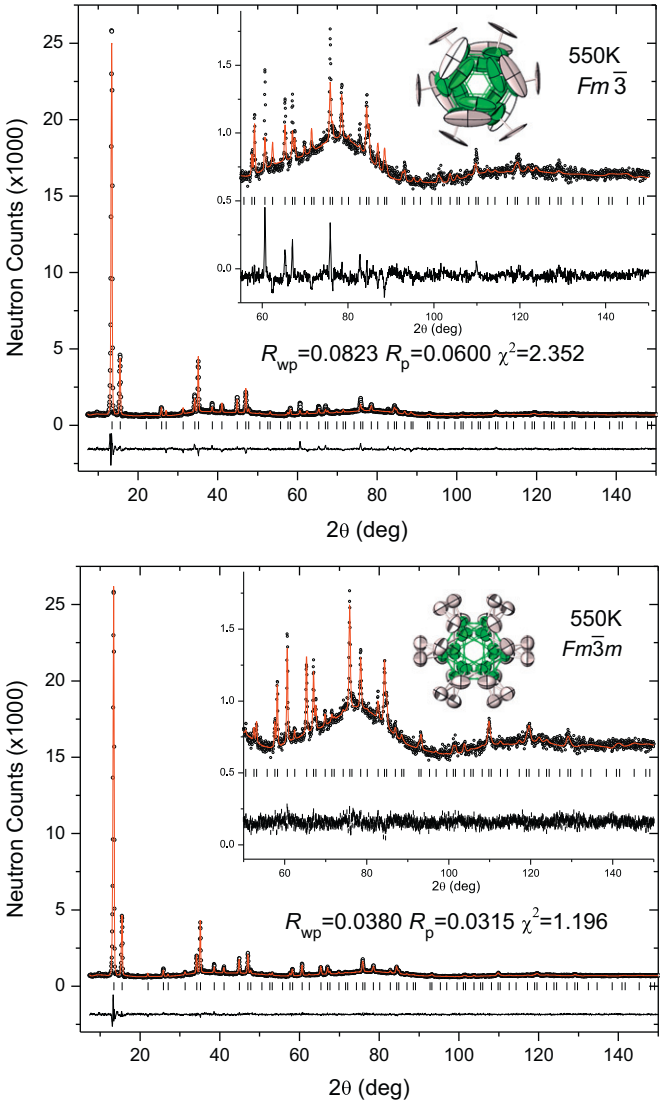

Fig. 4. Observed (circles), calculated (red lines), and difference profiles (beneath) of the Rietveld-refined 550 K NPD patterns for $Cs_2^{11}B_{12}D_{12}$ using the low-temperature $Fm\bar{3}$ structural model (top) and the disordered $Fm\bar{3}m$ structural model (bottom). Vertical bars denote the calculated Bragg peak positions. Uncertainties, not shown, are commensurate with the indicated scatter. In the inset, viewed down the [1 1 1] axis, are the corresponding anions defined by their thermal ellipsoids (green for B; white for D) resulting from each structural model. (For interpretation of the references to colour in this figure legend, the reader is referred to the web version of this article.)

(over a 17 K temperature range) for all three alkali-metal compounds with that of standard Zn and In melting-point transition peaks, we estimated relatively small enthalpy changes on the order of (50–270) J/mol $A_2B_{12}H_{12}$, the value decreases with an increase in cation radius. This is considerably less by an order of magnitude than the expected order–disorder transition enthalpy, $\Delta H = T\Delta S = RT \ln 2$, where $R \ln 2$ is the entropy change assuming complete configurational disorder [27]. This is a strong indication that the transition to complete disorder covers a larger temperature range than what has been integrated, and that some short-range anion order (over a 1–2 nm range) may still persist at and above the transition region. It should be noted that this coherence length would not be large enough to affect the expected Bragg peaks of the completely disordered structure model found to fit the high-temperature NPD patterns. This sort of behavior has previously been observed for the lambda transition of KBH_4, also apparently due to an incomplete order–disorder transition at the lambda point, which continues to completion over a much higher, larger temperature range [28,29].

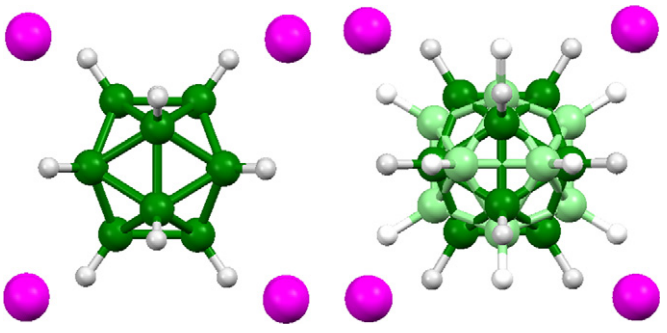

Fig. 5. Schematic viewed down the [1 0 0] axis of the (left) single, ordered orientation at low temperature and (right) two disordered orientations at high temperature of the $B_{12}D_{12}^{2-}$ icosahedral anion within the Cs_8 interstice. The two orientations for the latter are distinguished by different shades for the B and D atoms.

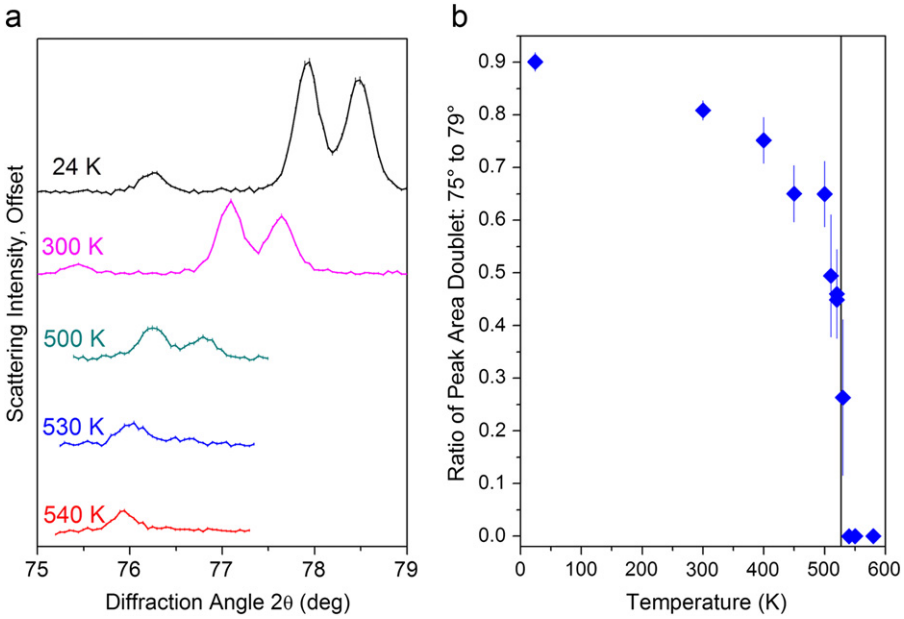

Fig. 6. (a) A doublet found in the low-temperature phase of $Cs_2^{11}B_{12}D_{12}$ with peaks at 77.9° and 78.4° 2θ at 24 K. The doublet shifts and changes in relative intensity as the sample is warmed to 540 K. (b) The ratio of the two peak areas of this doublet. (Vertical line marks 527 K.) Vertical error bars represent $\pm 1\ \sigma$.

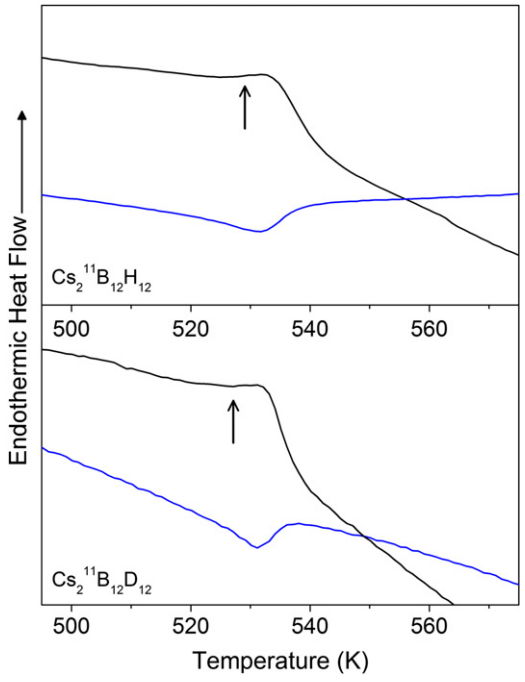

Fig. 7. The DSC measurements of $Cs_2^{11}B_{12}H_{12}$ (top) and $Cs_2^{11}B_{12}D_{12}$ (bottom) yielding transitions at 529 K and 527 K, respectively, based on the onset of the transition peak upon heating (black, 10 K/min) and denoted by arrows. The transition is reversible as demonstrated by the peak upon cooling (blue, uncontrolled temperature ramp). Uncertainties, not shown, are commensurate with the indicated scatter. (For interpretation of the references to colour in this figure legend, the reader is referred to the web version of this article.)

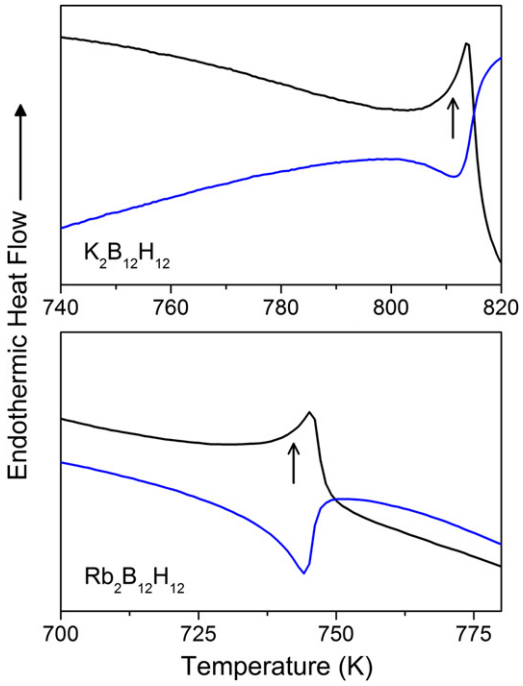

Fig. 8. DSC measurements of $K_2B_{12}H_{12}$ (top) and $Rb_2B_{12}H_{12}$ (bottom) yielding transitions at 811 K and 742 K, respectively, based on the onset of the transition peak upon heating (black, 10 K/min) and denoted by the arrows. The peak upon cooling (blue, uncontrolled temperature ramp) demonstrates the reversibility of the phase change. Uncertainties, not shown, are commensurate with the indicated scatter. (For interpretation of the references to colour in this figure legend, the reader is referred to the web version of this article.)

4. Conclusions

$Cs_2B_{12}H_{12}$ was found by NPD and DSC to undergo an order–disorder ($Fm\bar{3}$ to $Fm\bar{3}m$) phase transition near 529 K (527 K for $Cs_2B_{12}D_{12}$). Above this temperature, the cubic structure possesses a reorientational disordering of the icosahedral $B_{12}H_{12}^{2-}$ anions. A comparison of DSC measurements for $Cs_2B_{12}H_{12}$, $Rb_2B_{12}H_{12}$, and $K_2B_{12}H_{12}$ suggest similar transitions occur for all three compounds, although confirmation by NPD measurements is still required for the latter two. The presence of such an order–disorder transition should have interesting implications for the relative nature of the reorientational jump mechanism of the $B_{12}H_{12}^{2-}$ anions below and above the phase transition. We are currently investigating the effect of the transition on the anion dynamics with detailed quasielastic neutron scattering and NMR measurements over a broad temperature range. Also, the search for possible phase transitions is being

extended to the dodecahydro-*closo*-dodecaborate salts of Na and Li as well as the alkaline-earth metals.

Acknowledgments

This work was partially supported by the DOE through Award nos. DE-AI-01-05EE11104 and DE-AC04-94AL85000 within the EERE-supported Metal Hydride Center of Excellence.

Appendix A. Supplementary materials

Supplementary data associated with this article can be found in the online version at doi:10.1016/j.jssc.2011.09.010.

References

[1] D.G. Allis, B.S. Hudson, J. Phys. Chem. A 110 (2006) 3744–3749.
[2] N. Verdal, W. Zhou, V. Stavila, J.-H. Her, M. Yousufuddin, T. Yildirim, T.J. Udovic, J. Alloy. Compd. 509S (2011) S694–S697.
[3] I. Tiritiris, T. Schleid, Z. Anorg. Allg. Chem. 629 (2003) 1390–1402.
[4] R. Hoffman, W.N. Lipscomb, J. Chem. Phys. 36 (1962).
[5] S.-J. Hwang, R.C. Bowman, J.W. Reiter, J. Rijssenbeek, G.L. Soloveichik, J.-C. Zhao, H. Kabbour, C.C. Ahn, J. Phys. Chem. C 112 (2008) 3164–3169.
[6] V. Stavila, J.-H. Her, W. Zhou, S.-J. Hwang, C. Kim, L.A.M. Ottley, T.J. Udovic, J. Solid State Chem. 183 (2010) 1133–1140.
[7] J.-H. Her, M. Yousufuddin, W. Zhou, S.S. Jalisatgi, J.G. Kulleck, J.A. Zan, S.-J. Hwang, R.C. Bowman, T.J. Udovic, Inorg. Chem. 47 (2008) 9757–9759.
[8] J.-H. Her, W. Zhou, V. Stavila, C.M. Brown, T.J. Udovic, J. Phys. Chem. C 113 (2009) 11187.
[9] J.A. Wunderlich, W.N. Lipscomb, J. Am. Chem. Soc. 82 (1960) 4427.
[10] I. Tiritiris, T. Schleid, K. Müller, W. Preetz, Z. Anorg. Allg. Chem. 626 (2000) 323.
[11] I. Tiritiris, T. Schleid, K. Muller, Appl. Magn. Reson. 32 (2007) 459–481.
[12] N. Verdal, T.J. Udovic, J.J. Rush, R.L. Cappelletti, W. Zhou, J. Phys. Chem. A 115 (2011) 2933–2938.
[13] O.A. Babanova, A.V. Soloninin, A.P. Stepanov, A.V. Skripov, Y. Filinchuk, J. Phys. Chem. C 114 (2010) 3712–3718.
[14] A. Remhof, Z. Łodziana, P. Martelli, O. Friedrichs, A. Züttel, A.V. Skripov, J.P. Embs, T. Strässle, Phys. Rev. B 81 (2010) 214304.
[15] N. Verdal, M.R. Hartman, T. Jenkins, D.J. DeVries, J.J. Rush, T.J. Udovic, J. Phys. Chem. C 114 (2010) 10027–10033.
[16] P. Fischer, A. Züttel, Mater. Sci. Forum 443–444 (2004) 287–290.
[17] G. Renaudin, S. Gomes, H. Hagemann, L. Keller, K. Yvon, J. Alloy. Compd. 375 (2004) 98–106.
[18] The mention of all commercial suppliers in this paper is for clarity. This does not imply our recommendation or endorsement of these suppliers.
[19] K.A. Solntsev, N.T. Kuznetsov, V.I. Ponomarev, Inorg. Mater. 12 (1976) 874.
[20] J.K. Stalick, E. Prince, A. Santoro, I.G. Schroder, J.J. Rush, in: D.A. Neumann, T.P. Russell, B.J. Wuensch (Eds.), Neutron Scattering in Materials Science II, Materials Research Soc, Pittsburgh, 1995, pp. 101–106.
[21] H.M. Rietveld, J. Appl. Crystallogr. 2 (1969) 65.
[22] A.C. Larson, R.B.V. Dreele, General Structure Analysis System, Report LAUR 86-748 (Los Alamos National Laboratory, 1994).
[23] T.J. Udovic, C.M. Brown, J.B. Leão, P.C. Brand, R.D. Jiggetts, R. Zeitoun, T.A. Pierce, I. Peral, J.R.D. Copley, Q. Huang, D.A. Neumann, R.J. Fields, Nucl. Instr. Meth. A 588 (2008) 406–413.
[24] O. Charkin, Russ. J. Inorg. Chem. 52 (2007) 1746–1757.
[25] J.R.D. Copley, D.A. Neumann, R.L. Cappelletti, W.A. Kamitakahara, J. Phys. Chem. Solids 53 (1992) 1353–1371.
[26] I. Tiritiris, J. Weidlein, T. Schleid, Z. Naturforsch. 60b (2005) 627–639.
[27] W.H. Stockmayer, C.C. Stephenson, J. Chem. Phys. 21 (1953) 1311–1312.
[28] D.O. Welch, Masters Thesis, Massachusetts Institute of Technology, 1962.
[29] G.T. Furukawa, M.L. Reilly, J.H. Piccirelli, J. Res. NBS A 68 (1964) 651–659.